Extended self-similarity in boundary layer turbulence

G. Amati,[1] R. Benzi,[2] and S. Succi[3]
[1]*Dipartimento di Meccanica e Aeronautica, Università ''La Sapienza,'' Via Eudossiana 18, I-00184 Roma, Italy*
[2]*Dipartimento di Fisica, Università ''Tor Vergata,'' Via E. Carnevale, I-00173 Roma, Italy*
[3]*Istituto Applicazioni Calcolo ''M. Picone,'' Via del Policlinico 137, I-00161 Roma, Italy*
(Received 26 December 1996)

It is shown that a lack of isotropy narrows the range of spatial scales where turbulent flows exhibit extended self-similarity (ESS), namely, self-scaling of velocity structure functions. This effect holds irrespectively of the order of the structure functions and explains why early experiments on turbulent boundary layers failed to observe ESS. The shrinking of the ESS range of scales is well captured by the approximate analytical scaling functions developed by Sreenivasan and co-workers [Phys. Rev. E **48**, R33 (1993); **48**, 5 (1993); **48**, R3217 (1993)] to fit atmospheric boundary layer data. [S1063-651X(97)04806-X]

PACS number(s): 47.27.−i, 47.10.+g

Recently, the existence of an extended form of scale invariance [extended self-similarity (ESS)] in fluid flows has been pointed out [1]. ESS consists in representing the pth-order structure function of the velocity field S_p not in terms of the space separation r, but as a function of the third-order (or any other order) structure function S_3 instead. The rationale behind this idea is that the structure functions exhibit a generalized form of scale *self-invariance* that holds even at low Reynolds number, i.e., when dissipative effects still affect the dynamics of the turbulent flow.

Formally, ESS reads as

$$S_p(r) \simeq S_q(r)^{\zeta_p/\zeta_q}, \tag{1}$$

where $S_p(r) \equiv \langle \delta v(r)^p \rangle$ is the pth-order longitudinal velocity structure function (with r aligned with $\vec{v}$) and $\delta v(r) = |\vec{v}(x+r) - \vec{v}(r)|$ is the variation of the velocity field taken at two locations a distance r apart. Angular brackets denote ensemble averaging and ζ_p are the scaling exponents of the velocity field fluctuations.

Since for most flows $\zeta_3 = 1$, the above relation identifies S_3 as a sort of natural generalized space coordinate capable of tracking self-similarity even when dissipative effects would hide it to the ''naive'' metric represented by the space separation r.

According to the Kolmogorov relation [2]

$$S_3(r) = -\frac{4}{5}\langle \epsilon \rangle r + 6\nu \frac{dS_2}{dr}, \tag{2}$$

when molecular viscosity becomes vanishingly small ($\nu \to 0$), while turbulent dissipation stays finite ($\epsilon > 0$), S_3 becomes proportional to the space separation r so that ''conventional'' self-similarity is recovered.

ESS departs from previous scaling theories in at least three respects [2,3]. (i) It holds also at moderately low Reynolds numbers. This contrasts with ordinary scaling, which assumes fully developed turbulence. A theoretical explanation of this experimental and numerical evidence is still awaiting a final assessment [4]. (ii) It survives down to mildly supradissipative scales of the order of 5η, where $\eta = \nu^{3/4}\epsilon^{-1/4}$ is the Kolmogorov length. This contrasts with ordinary scaling, which is known to fade away at much larger scales, of the order of 30η or more [5,6]. (iii) It shows anomalous scaling, i.e., scaling exponents departing from linear non-intermittent behavior $\zeta_p = p/3$, all the way down to $r = 5\eta$.

Other numerical and experimental studies supporting ESS have also been reported [4]. Nevertheless, some early criticism has been raised [7]. In particular, it has been argued that ESS may bear little relevance to fluid turbulence in that relation (1) would break down as soon as the order p is made sufficiently high.

In this paper we argue that the failure to observe ESS in boundary layer turbulence is by no means related to high p's, but results rather from the lack of isotropy of the flow, i.e., directional effects such as those typically associated with shear and boundary-layer flows.

Four distinct data sets have been inspected to back up this statement: (i) The jet flow experiment (J, $\mathrm{Re}_\lambda \simeq 800$) [8], (ii) the numerical simulation of homogeneous incompressible turbulence (H; $\mathrm{Re}_\lambda \simeq 38$) [9], (iii) the atmospheric boundary layer experiment (A; $\mathrm{Re}_\lambda \simeq 190$) [7], and (iv) the numerical simulation of turbulent channel flow (C; $\mathrm{Re}_\lambda \simeq 65$) [10]. This sample of data sets allows several cross-checks since it offers all four combinations of experimental (J,A) versus numerical (H,C) and isotropic (J,H) versus nonisotropic (A,C) situations.

Full details pertaining to data sets J,H,A can be found in the original papers. Therefore, here we shall report only some information concerning the channel flow simulation (case C).

The simulation is based on a lattice Boltzmann (LB) code, suitably generalized to accommodate a nonuniform Cartesian mesh [10]. The LB code has been run on a moderate resolution grid ($64 \times 64 \times 128$) covering a physical length of $920 \times 512 \times 192$ lattice units along the streamwise (x), spanwise (z), and normal-to-wall (y) directions. The spatial extent of the domain is large enough to sustain the streamwise rolls fueling cross-channel turbulence [11]. The simulation spans 2.4×10^5 time steps, corresponding to about 90 streamwise recirculation times.

Data slices are sampled every 50 time steps in the interval $[10^5, 2.4 \times 10^5]$ at three different elevations $y^+ = 5$ (inside

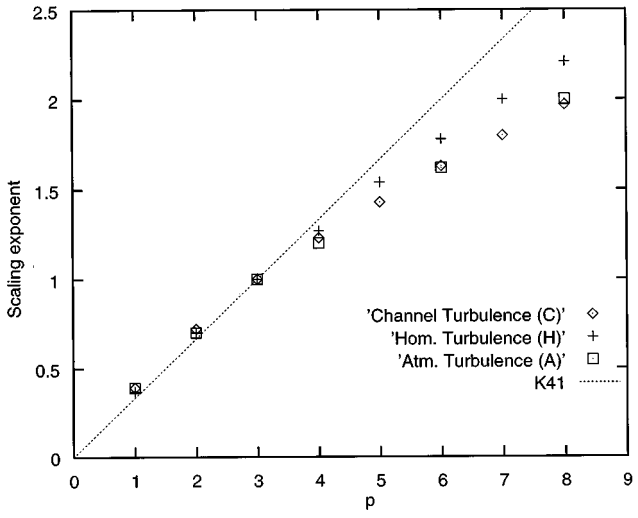

FIG. 1. Scaling exponent ζ_p as a function of p for homogeneous isotropic incompressible turbulence (H), channel flow turbulence at $y^+=25$ (C), and atmospheric boundary layer (A).

the viscous sublayer right above the bottom wall), $y^+=25$ (within the transition layer), and $y^+=50$ (inside the logarithmic layer). This corresponds to about 10^7 samples per plane. Here y^+ is the normal-to-wall distance normalized with the shear wall velocity v^* and the molecular viscosity ν, $y^+=yv^*/\nu$. The LB code takes about 5 CPU sec/step on a midrange superscalar work-station and performs competitively with more consolidated numerical methods for channel flow turbulence.

In Fig. 1 we report the scaling exponent ζ_p as a function of p ($p\leqslant 8$) for datasets H,A,C. Our data refer to the plane at $y^+=25$. A preliminary remark is that anisotropic flows (A,C) are significantly more intermittent than the isotropic one (H). This is likely to result from the systematic ejection of coherent structures carrying conspicuous fluctuations from (to) the wall layer to (from) the bulk flow (see Fig. 2).

A second remark concerns the excellent match between ζ_p^A and ζ_p^C in spite of the (apparently) disparate nature of the corresponding flows: numerical simulation of channel flow at $\mathrm{Re}_\lambda\simeq 65$ for case C and experimental data of boundary layer turbulence at $\mathrm{Re}_\lambda\simeq 190$ for case A.

This indicates that, as far as anomalous scaling is concerned, flows A and C can be regarded as two distinct but equivalent realizations within the same *class* of flows. Thus we shall use flow C to understand why flow A was apparently showing no sign of ESS.

To focus on this issue we concentrate on the sixth-order scaling exponent, namely, the one displaying the best match between flows A and C. The conclusion we shall arrive at applies, however, to the fourth- and eighth-order exponents as well.

We compute the corresponding scaling exponent ζ_6 by plotting S_6 versus S_3. More precisely, we examine the local exponent ζ_6 by plotting the local slope

$$s_6(r)=\frac{dS_6}{dS_3^{\zeta_6}} \tag{3}$$

as a function of r, the idea being that departures of $s_6(r)$ from a constant value would signal the loss of ESS behavior.

The function $S_6(r)$ is reported in Fig. 3 for all four datasets under inspection. The numerically computed values are $\zeta_6\simeq 1.78$ for isotropic flows and $\zeta_6\simeq 1.62$ for the nonisotropic ones, in reasonable agreement with the existing literature [3].

The way these figures are obtained deserves some comment. First, a clear-cut separation between the behavior of isotropic (J,H) versus anisotropic (A,C) datasets is apparent. The isotropic datasets follow a flat profile down to scale separations as low as about 5η (note that we plot r/η on

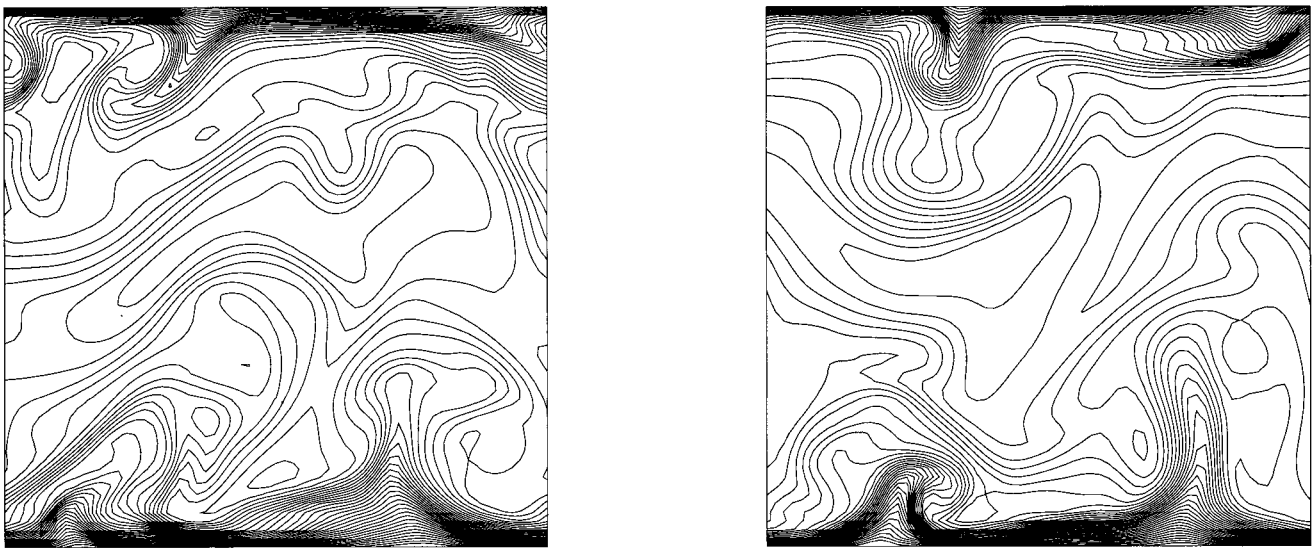

FIG. 2. Coherent structures ejected from the wall boundary layer in a turbulent channel flow simulation. The normal-to-wall (y) direction is the ordinate and the spanwise (z) direction is the abscissa. The two pictures represent the isocontours of the streamwise velocity in two planes orthogonal to the mean flow (down into the page) after a few hundred longitudinal recirculation times. The two sections are located at the channel inlet (left) and $\frac{3}{4}$ channel length (right) along the streamwise direction (x).

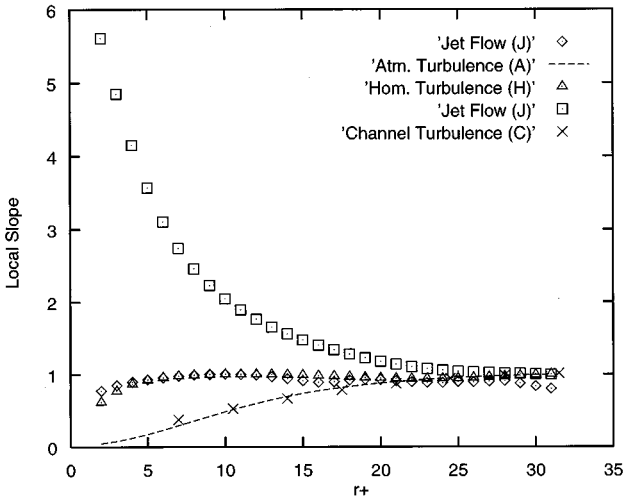

FIG. 3. Computation of the sixth-order scaling exponent ζ_6 from local slopes of $S_6(r)$ versus $S_3(r)$. The local slope (ordinate) is reported as a function of $r^+=r/\eta$ (abscissa). Squares, dS_6/dS_3^2, case *J*; diamonds, $dS_6/dS_3^{1.78}$, case *J*; triangles, $dS_6/dS_3^{1.78}$, case *H*; dashed line, $dS_6/dS_3^{1.62}$, best-fit scaling function, case *A*; crosses, $dS_6/dS_3^{1.62}$, case *C*. The squares show a manifest departure from that of [2], i.e., intermittency. Curves *J*,*H* (isotropic flows) display flat behavior (a signature of ESS) down to about 5η, while for anisotropic flows ESS fades away below 25η. This shows that a lack of isotropy spoils ESS for low-order structure functions.

abscissas). This is a typical signature of ESS behavior and shows that the numerical computation of ζ_p for these flows can be improved by using data in the near-dissipative regime.

Anisotropic datasets, on the contrary, do show significant departures from a flat profile, i.e., non-ESS behavior, already starting at $r\simeq 25\eta$. This means that the scaling exponents for these flows must be computed either by using data from the inertial regime alone, above 25η, or by resorting to best-fit scaling functions smoothly connecting the inertial and dissipative regimes. These functions have been obtained in [12] by optimal interpolation of atmospheric boundary layer data using expressions of the form given by Eq. (6).

This proves that, *even at low p*, directional effects (as opposed to high *p*'s) are responsible for the ''disappearance'' of ESS behavior. Again the striking feature is that both anisotropic datasets deviate from ESS along basically the *same* curve. Let us emphasize that, given the fact that we are dealing with widely distinct Reynolds numbers and fairly subtle observables, namely, derivatives of structure functions, such an agreement can hardly be regarded as a mere coincidence.

Returning to ESS, we wish to point out that a lack of isotropy does *not* destroy ESS altogether, but only narrows its range of scales. In particular, the shortest scale where ESS is detectable is shifted towards larger scales in the inertial regime $r\simeq 25\eta$. Backed by the findings described in [13,14], we are naturally led to interpret this loss of ESS as a destructive interference induced by structures at a typical boundary layer scale δ. This is indeed the case for the experimental data discussed in Ref. [7], where ESS was probed by using data well inside the turbulent boundary layer. This interference can be formalized by postulating a double-scaling expression for the structure functions of the form

$$S_p(r)=A_pU_0^p\left[\frac{r}{L}\,f\left(\frac{r}{\eta}\right)\right]^{\zeta_p}g\left(\frac{r}{\Lambda}\right)^{\chi_p},\quad r>r_1, \tag{4}$$

where A_p is a normalization constant, U_0 is a typical large-scale speed, and $r_1\simeq 5\eta$. By definition, the function $f(r)\to 1$ in the limit $r\gg r_1$ in such a way as to recover the usual Kolmogorov scaling.

Based on the data presented in Fig. 3, the ''interference function'' $g(r)$ should comply with the requirement $g(r)\to 1$ for $r>\Lambda>r_1$, so as to break ESS only for scales $r<\Lambda$. Here Λ is a spatial cutoff bearing a (yet unknown) relation to the boundary layer thickness δ.

It should be noted that the double scaling (4), while breaking ESS (for $r<\Lambda$ only), is still compatible with more general forms of scaling. To this purpose, let us define *relative* scaling functions in the form $G_p\equiv S_p(r)S_3(r)^{\alpha_p}$, with $\alpha_p=\zeta_p+\chi_p$. Simple algebra yields

$$G_p(r)=G_q(r)^{\mu_{p3}/\mu_{q3}}, \tag{5}$$

where $\mu_{pq}=\zeta_p\chi_q-\zeta_q\chi_p$ is the two-point commutator associated with the scaling exponents ζ_p and χ_p. Note that the generic commutator identically vanishes if the scaling exponents are linear functions of the indices p,q. This is why scaling laws in the form (5) are particularly suited to probe universal features of intermittent phenomena.

Expression (5) is nothing but a generic instance of the so-called generalized ESS (GESS) recently introduced by Benzi, Struglia, and Tripiccione in the context of anisotropic shear flows [13]. In particular, GESS is recovered from Eq. (5) whenever the interference field $g(r)$ scales nonintermittently, i.e., $\chi_p=p\chi_3/3$. Indeed, evidence of GESS has been reported for a variety of flows, including those discussed in this paper. It is worth noting that the analytical scaling functions developed in [7,15] to interpret boundary layer experiment also fall within the class described by expression (4). In fact, these scaling functions can be expressed in the form

$$F_p(r)=(r/\eta)^{2p}[1+B_p(r/\eta)^2]^{-C_p}, \tag{6}$$

where $C_p=2p-\zeta_p$, and recall that the constants B_p, controlling the viscous-to-inertial transition scale, are nearly independent of p ($1/B_p^{1/2}\simeq 11$). In view of this, it comes as no surprise that these analytical scaling functions, although calibrated for the atmospheric boundary layer experiment, work pretty well also for the interpretation of our turbulent channel data.

Summarizing, we have presented numerical and experimental evidence supporting the idea that a lack of isotropy shrinks the range of scales where ESS can be detected. This effect takes place irrespectively of the order of the structure functions under inspection and is captured well by (approximate) analytical scaling functions smoothly connecting the inertial and dissipative regimes.

We wish to acknowledge Professor R. Piva for several illuminating discussions.

[1] R. Benzi, S. Ciliberto, R. Tripiccione, F. Massaioli, C. Baudet, and S. Succi, Phys. Rev. E **48**, R29 (1993)
[2] A. Kolmogorov, C. R. Acad. Sci. USSR **30**, 301 (1941); **30**, 1 (1941).
[3] U. Frisch, *Turbulence, The Legacy of A.N. Kolmogorov* (Cambridge University Press, Cambridge, 1995).
[4] R. Benzi, L. Biferale, S. Ciliberto, M. V. Struglia, and R. Tripiccione, Physica D **96**, 162 (1996).
[5] Z. S. She and E. Waymire, Phys. Rev. Lett. **74**, 262 (1995).
[6] Z. S. She, S. Chen, G. Doolen, R. Kraichnan, and S. Orszag, Phys. Rev. Lett. **72**, 344 (1994).
[7] G. Stolovitzky and K. Sreenivasan, Phys. Rev. E **48**, R33 (1993).
[8] C. Baudet, S. Ciliberto, and P. Thien, J. Phys, (France) II **3**, 293 (1993).
[9] M. Briscolini, P. Santangelo, S. Succi, and R. Benzi, Phys. Rev. E **50**, 1745 (1994).
[10] G. Amati, S. Succi, and R. Benzi, Fluid Dyn. Res. (to be published).
[11] P. Moin and J. Kim, J. Fluid Mech. **177**, 133 (1987).
[12] G. Stolovitzky, K. Sreenivasan, and A. Juneja, Phys. Rev. E **48**, 5 (1993); **48**, R3217 (1993).
[13] R. Benzi, M. V. Struglia, and R. Tripiccione, Phys. Rev. E **53**, R6 (1996).
[14] R. Benzi, L. Biferale, S. Ciliberto, M. V. Struglia, and R. Tripiccione, Europhys. Lett. **32**, 9 (1995); **32**, 709 (1995).
[15] L. Sirovich, L. Smith, and V. Yakhot, Phys. Rev. Lett. **70**, 3251 (1993).